Modified reflection in birefringent layers of core-shell semiconductor nanowires

S L Diedenhofen and J Gómez Rivas

FOM Institute for Atomic and Molecular Physics AMOLF, Center for Nanophotonics, c/o Philips Research Laboratories Eindhoven, High Tech Campus 4, 5656 AE Eindhoven, The Netherlands

E-mail: `diedenhofen@amolf.nl`

Abstract. Birefringent layers of GaP nanowires are grown by metal-organic vapor phase epitaxy on top of a GaP substrate. We modified the reflection of the as-grown layer by adding a shell of 12 nm of SiO_2 around the nanowires. The effect of the shell on the effective refractive indices of the birefringent nanowire layer was calculated using Maxwell-Garnett effective medium theory for coated cylinders. The large change of the reflection due to the shell renders nanowire layers a promising material for sensing applications.

PACS numbers: 42.25Lc, 81.05.Ea, 78.67.Lt

Submitted to: *Semicond. Sci. Technol.*

1. Introduction

Optical properties of semiconductor nanowires have been studied extensively over the last years [1–8]. Lasing [1], LED's [2], and photosensitive devices [3] have been demonstrated on single nanowires. Ensembles of nanowires are recognized as promising materials for large area LED's [4], anti-reflection coatings [5], and photoelectrochemical cells [6]. Due to the large geometrical anisotropy of individual nanowires, ensembles of nanowires may exhibit giant optical birefringence [7]. Here, we demonstrate that the specular reflection of birefringent layers of GaP nanowires can be modified by adding a shell of SiO_2 around them. We have measured with s- and p-polarized light and found that the s-polarized reflection is more affected by the shell. The larger sensitivity of s-polarization to changes in the nanowire surrounding is described by calculations using the Maxwell-Garnett effective medium theory for coated cylinders [9] and the Jones calculus [10].

Over the last decade, porous systems have attracted much attention in the fields of gas-, bio-, or chemical sensors [11–21]. Porous structures are very sensitive due to a large surface to volume ratio. Recent works on porous silicon have shown that the reflection [11] and transmission [12] as well as the birefringence [13] are modified by infiltrating the pores with DNA [14], proteins [15], or gases [16]. In principle, all these sensors have one thing in common: They detect a change of the refractive index of the material filling the pores. In contrary to works on porous materials, we focus here on a direct and open structure based on bottom-up processed semiconductor nanowires. Direct structures can be easily infiltrated with a material to be sensed. The large birefringence of the nanowire layers, together with the large surface to volume ratio, leads to a high sensitivity of the reflection or transmission of light to a material surrounding the wires. We have chosen to work with SiO_2 as the material forming the nanowire shell because of the similar refractive index compared to biomolecules [22].

The manuscript is organized as follows: We explain the growth of the nanowire layers in section 2. Section 3 presents the optical reflection measurements from ensembles of nanowires. In section 4 we discuss the effective refractive indices for s- and p-polarization of the nanowire layer and their dependence on the refractive index surrounding the wires. The manuscript ends with the conclusions.

2. Sample fabrication and characterization

High density vertically aligned GaP nanowires are grown on a GaP wafer in the vapor-liquid-solid (VLS) growth mode [23] in a metal-organic vapor phase epitaxy (MOVPE) reactor. After a cleaning step of the wafer in HNO_3:HCL:H_2O (2:3:3) at 80 °C for 2 min, a thin gold film with a thickness of 0.3 nm was deposited on the (111)B GaP substrate surface side (P-terminated). This gold film acts as a catalyst for the nanowire growth. During heating the gold film breaks up into small islands which form individual catalyst droplets from which the nanowires grow selectively. The nanowires are grown

for 17 min in the VLS-growth mode at a temperature of 420 °C in a low-pressure (50 mbar) MOVPE system (Aixtron 200) using trimethylgallium (TMG) and phosphine (PH_3) with molar fractions of $\chi_{\mathrm{TMG}} = 9.1 \cdot 10^{-5}$ and $\chi_{\mathrm{PH3}} = 15 \cdot 10^{-3}$, as precursors in a total flow of 6 l/min using hydrogen (H_2) as carrier gas. By increasing the temperature to 630 °C , where the kinetic hindrance for growth on the sidewalls is overcome, a shell is grown around the nanowires for 350 s to increase the filling fraction of GaP in the layer. After growth, the samples were cooled down in a PH_3 containing atmosphere. We cleaved the sample into two pieces, and left one half as grown as reference sample. On the other half SiO_2 is evaporated by plasma enhanced chemical vapor deposition (PECVD) at a temperature of 300 K and a pressure of 2.4 Torr for 10 s.

Although we focus here on GaP nanowires grown on a GaP substrate, comparable structures can be fabricated using any group IV [24], III/V [2, 4, 8, 25], or II/VI [26, 27] semiconductor material allowing an easy functionalization of the surface depending on the material to detect.

Figure 1a shows a side view scanning electron micrograph (SEM) of the nanowire sample as grown. From this image, the length of the nanowires can be estimated to be 1.26 μm $\pm$ 0.1 μm and the diameter to be 40 nm $\pm$ 25 nm. In Figure 1b a transmission electron micrograph (TEM) of a nanowire covered with 12 nm of SiO_2 is shown. It is remarkable that the SiO_2 shell has a constant thickness over the nanowire length, which indicates a good infiltration of the layer. The core of the nanowire shows twinning defects, with alternating orientations along the $< 111 >$ axis of the wire, and the gold particle used to catalyze the growth of the wires is visible on top of the nanowire. Both the twinning defects and the gold particle have no significant effect on the optical properties discussed next [7, 28].

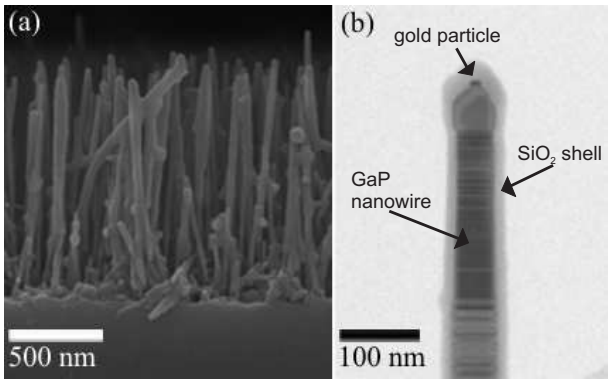

Figure 1. a) Side view scanning electron micrograph of as grown nanowires. b) Transmission electron micrograph of a nanowire coated with SiO_2.

3. Optical Measurements

We have measured spectra of the angular dependent specular reflection of ensembles of vertically aligned nanowires on a GaP substrate. The nanowire sample was illuminated

using a collimated beam from a halogen white-light source, while the sample and the detector were mounted on computer-controlled rotational stages. For detecting the light in the visible (410 nm - 900 nm), a spectrometer with a silicon detector (Ocean Optics, USB2000) is used. The infrared signal (900 nm - 1610 nm) is measured using an InGaAs CCD camera (Andor iDUS).

Figure 2 shows specular reflection spectra for s- and p-polarized incidence measured at an angle of incidence of 60 °. From the Fabry-Pérot oscillations visible in both measurements, we can conclude that the nanowire layer acts as an optical cavity due to the contrast of refractive indices at the air-nanowire and the nanowire-substrate interfaces. The reflection is reduced for photon energies above 1.77 eV ($\lambda = 700$ nm) due to Rayleigh scattering in the layer [28]. For energies above 2.25 eV ($\lambda = 550$ nm), the reflection is further reduced due to absorption in GaP. The noise in the measurememts at wavelengths around 900 nm is related to the low quantum efficiency of the Si- and InGaAs-detectors in this wavelength range. Due to birefringence, the nanowire layer exhibits a larger optical thickness for p-polarized light than for s-polarized light, i.e., the effective refractive index for p-polarized light is larger than for s-polarized light. This difference in path length is apparent in the different period of the Fabry-Pérot oscillations of Figure 2. Figure 2b shows a calculation of the reflection performed using Jones calculus [10]. From these calculations, the ordinary n_o and extraordinary n_e refractive indices of the nanowire layer can be determined to vary from 1.10 to 1.12 and from 1.28 to 1.93, respectively, for photon energies ranging from 0.77 eV to 3.0 eV (1610 nm to 413 nm). The ordinary refractive index n_o corresponds to the refractive index for light polarized perpendicular to the nanowire long axis, while n_e describes the refractive index for for light polarized parallel to this axis. The refractive index for s-polarization equals the ordinary refractive index. This polarization is always perpendicular to the nanowire long axis. P-polarized light has a component along the long axis of the nanowires and a component perpendicular to this axis dependent on the angle of incidence. The refractive index for p-polarization is related to the ordinary and extraordinary refractive indices by [29]

$$n_\mathrm{p} = \sqrt{n_\mathrm{o}^2 + \frac{n_\mathrm{e}^2 - n_\mathrm{o}^2}{n_\mathrm{e}^2} \cdot \sin^2\theta}. \tag{1}$$

For an angle of incidence θ of 60°, n_s ranges from 1.10 to 1.12 and n_p from 1.19 to 1.32.

Figure 3a and b display the specular reflection of s-polarized light from the uncoated nanowire sample and the sample with a thin shell of SiO_2, respectively, as a function of wavelength and angle of incidence. A shift of the Fabry-Pérot oscillations to larger wavelengths for the coated nanowires is visible. For clarity, Figures 3c and d show measurements performed at an angle of incidence of 60 ° for s- (a) and p-polarization (b) for nanowire layers without and with a layer of SiO_2. In both cases, a clear shift of the Fabry-Pérot oscillations to lower energies (larger wavelengths) is visible, due to the increased optical thickness of the nanowire layer. The shift of the Fabry-Pérot

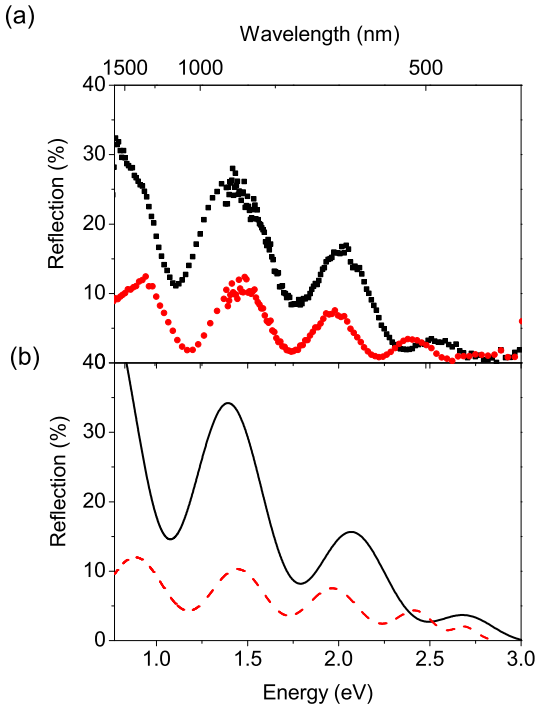

Figure 2. a) Measured specular reflection spectra from a layer of nanowires using s- (black squares) and p-polarized white light (red circles) for an angle of incidence of 60° and b) calculations performed using Jones calculus for an angle of incidence of 60° for s- (black solid curve) and p-polarized (red dashed curve) light.

oscillations depends on the wavelength and is larger for s- than for p-polarization. For s-polarization and an angle of incidence of 60°, a shell of 12 nm of SiO_2 around the nanowires shifts the signal by 105 nm.

The difference between the specular reflection measured on the nanowires covered with SiO_2 and without shell is shown in Figure 4a for an angle of incidence of 60 °, and for s- and p-polarized light. This difference is larger for s-polarization indicating that measurements with s-polarization are more sensitive to detect changes in the refractive index around the wires. Figure 4b displays calculations of the difference of the reflection spectra of a nanowire layer with and without SiO_2 shell. The calculations show a good agreement with the measurements confirming the enhanced sensitivity of s-polarization to changes in the surroundings of the nanowires.

The refractive index of SiO_2 in the visible and near infrared (n = 1.45) is similar to the refractive index of biomolecules [22]. Therefore, our results indicate that layers of semiconductor nanowires can be used for sensitive bio-sensors.

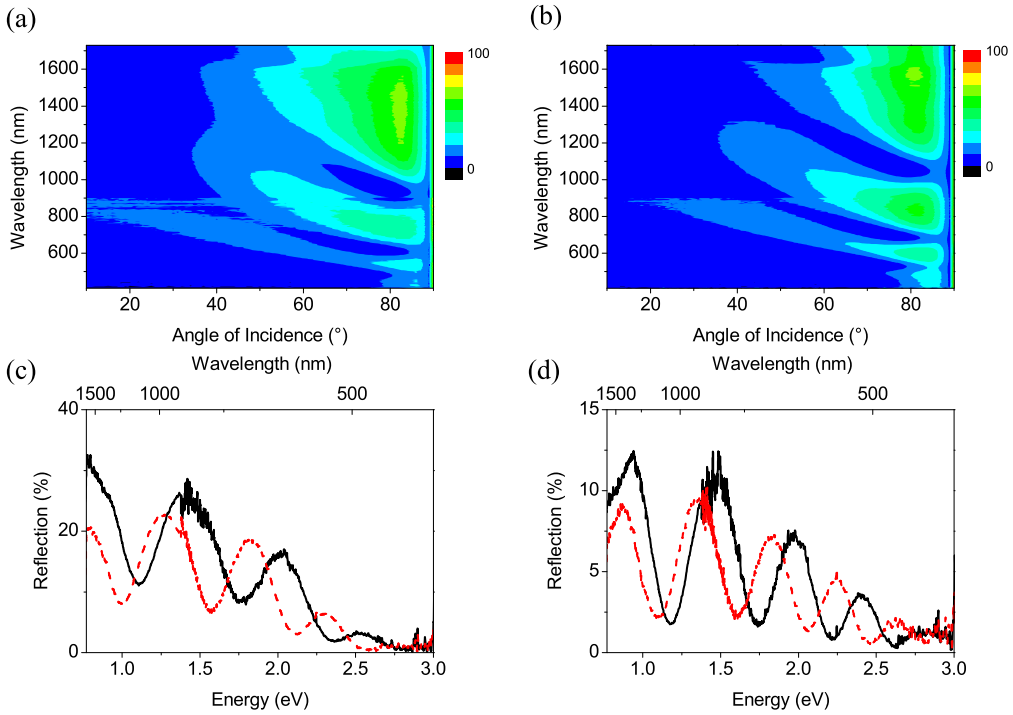

Figure 3. Measured specular reflection spectra of a layer of nanowires without a) and with b) a shell of 12 nm of SiO_2 around the nanowires using s-polarized white light as a function of the angle of incidence. Reflection spectra measured at an angle of incidence of 60° for c) s- and d) p-polarized light without shell (black solid curve) and with shell (red dashed curve).

4. Discussion

The larger wavelength shift of the reflection of light from layers of nanowires without and with a shell of SiO_2 for s-polarized light can be described by calculating the effect of a shell surrounding the wires on the effective refractive indices of the layer. The refractive index of s-polarized light n_s, which equals the ordinary refractive index n_o, is calculated using the Maxwell-Garnett effective medium theory for core-shell cylinders, [9]

$$n_s = n_o = (1 - \frac{2f_{cs}}{\gamma_1 + f_{cs}})^{\frac{1}{2}} \tag{2}$$

with

$$\gamma_1 = \frac{r_c^2(\epsilon_s - \epsilon_c)(\epsilon_{air} - \epsilon_s) + r_s^2(\epsilon_s + \epsilon_c)(\epsilon_{air} + \epsilon_s)}{r_c^2(\epsilon_s - \epsilon_c)(\epsilon_{air} + \epsilon_s) + r_s^2(\epsilon_s + \epsilon_c)(\epsilon_{air} - \epsilon_s)} \tag{3}$$

with r_c the radius and ϵ_c the refractive index of the core, r_s the radius of the core/shell nanowire and ϵ_s the refractive index of the shell, surrounded by air. The filling fraction of the coated nanowires is calculated using $f_{cs} = \pi r_s^2/d_{nw}^2$ with d_{nw} the

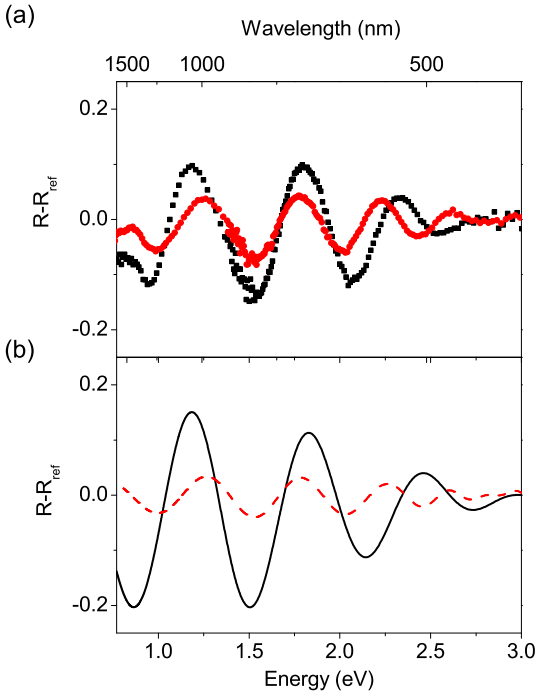

Figure 4. Difference between the specular reflection spectrum of the nanowire layer covered with a shell of 12 nm of SiO_2 and the layer of nanowires without shell for a) s- (black squares) and p-polarized light (red circles) measured at 60 ° and b) calculations of this difference for s-polarization (black solid curve) and p-polarization (red dashed curve).

distance between the midpoints of two nanowires. The extraordinary refractive index is calculated as the geometrical average of the three media [30]

$$n_{\mathrm{e}} = \sqrt{f_{\mathrm{c}}\epsilon_{\mathrm{c}} + f_{\mathrm{s}}\epsilon_{\mathrm{s}} + (1 - f_{\mathrm{c}} - f_{\mathrm{s}})\epsilon_{\mathrm{air}}} \tag{4}$$

with $f_{\mathrm{c}} = \pi r_{\mathrm{c}}^2/d_{\mathrm{nw}}^2$ and $f_{\mathrm{s}} = f_{\mathrm{cs}} - f_{\mathrm{c}}$.

From the ordinary, n_{o}, and the extraordinary, n_{e}, refractive indices, the refractive index for p-polarized light can be calculated with equation [1].

Figure 5a shows the refractive indices for s- and p-polarized light as a function of shell radius. This calculation has been done considering $d_{\mathrm{nw}} = 120$ nm, $r_{\mathrm{c}} = 20$ nm, $\epsilon_{\mathrm{s}} = n_{\mathrm{SiO_2}}^2 = 2.1$, $\epsilon_{\mathrm{c}} = n_{\mathrm{GaP}}^2 = 10.9$, and for an angle of incidence of 60 °. These parameters describe the sample discussed in Section 3. Note that the values of n_{s} and n_{p} for the nanowire layer without shell ($n_{\mathrm{s}} = 1.07$, $n_{\mathrm{p}} = 1.2$ at 633 nm) obtained from this model deviate from the experimental values ($n_{\mathrm{s}} = 1.11$, $n_{\mathrm{p}} = 1.21$). The theoretical values are calculated assuming infinitely long and perfectly aligned cylinders. However, the nanowires used in our experiments are bend and finite in size (see Figure 1), which leads to a reduction of the birefringence [7, 31], i.e. the ordinary refractive index increases while the extraordinary refractive decreases due to the misalignments. Figure 5b shows a calculation of the difference between the effective refractive index of

a layer of nanowires with a SiO_2 shell and without a shell as a function of the SiO_2 thickness. From Figure 5b, we can conclude that the refractive index for s-polarized light is more sensitive to changes of the surrounding than the refractive index for p-polarization in layers of GaP nanowires with the parameters described above. This higher sensitivity for s-polarized light gets larger for thicker shells. Furthermore, from Figure 5b we can estimate an increase of the effective refractive index for s-polarized light by 0.06 and for p-polarized light by 0.05 due to a 12 nm thick shell. As we have seen, these small changes have a strong impact on the specular reflection from the layers without and with a SiO_2 shell.

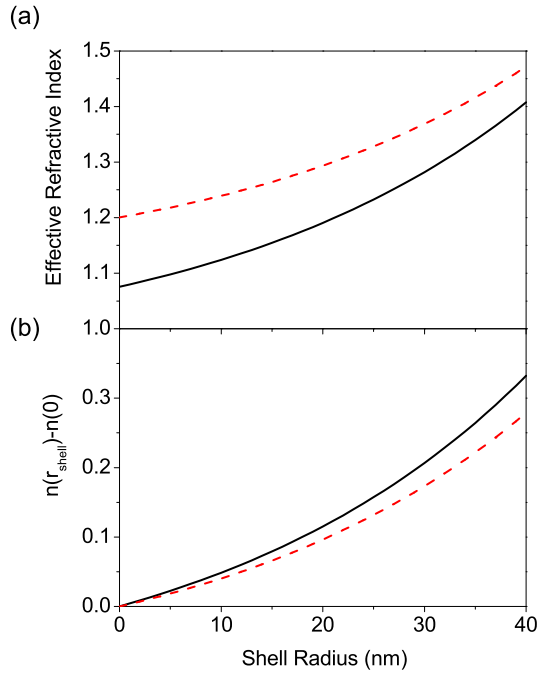

Figure 5. a) Effective refractive indices for s- (black solid curve) and p-polarization (red dashed curve) of a GaP nanowire layer as a function of the thickness of a shell around the nanowires with a refractive index of 1.45. The angle of incidence in this calculation is 60 °. b) Difference between the refractive indices without and with a shell as a function of the shell thickness.

5. Conclusions

We have demonstrated that the specular reflection from birefringent layers of semiconductor nanowires can be significantly modified by a SiO_2 shell as thin as 12 nm. We have compared the modification of the reflection for s- and p-polarized light. Due to the large birefringence of the nanowire layer, s-polarized reflection is more affected by the thin shell. This result is explained with the Maxwell-Garnett effective medium theory for coated cylinders. Our results indicate that a higher sensitivity can be achieved in birefringent porous systems by measuring with s-polarized light.

Acknowledgments

We thank G. Immink, M. T. Borgström, and E. P. A. M. Bakkers for the growth of the nanowires, E. Evens and R. van de Laar for technical assistance, F. Holthuysen for SEM analysis, M. A. Verheijen for TEM analysis and A. Hartsuiker for useful discussions. This work is part of the research program of the "Stichting voor Fundamenteel Onderzoek der Materie (FOM)", which is financially supported by the "Nederlandse organisatie voor Wetenschappelijk Onderzoek (NWO)" and is part of an industrial partnership program between Philips and FOM.

References

[1] Johnson J C, Choi H J, Knutsen K P, Schaller R D, Yang P and Saykally R J 2002 *Nature Materials* **1** 106–110

[2] Duan X, Huang Y, Cui Y, Wang J and Lieber C M 2001 *Nature* **409** 66–69

[3] Wang J, Gudiksen M S, Duan X, Cui Y and Lieber C M 2001 *Science* **292** 1455–1457

[4] An S J and Yi G C 2007 *Appl. Phys. Lett.* **91** 123109

[5] Diedenhofen S L, Vecchi G, Algra R E, Hartsuiker A, Muskens O L, Immink G, Bakkers E P A M, Vos W L and Rivas J G 2009 *Adv. Mat.* **21** 973–978

[6] Goodey A P, Eichfeld S M, Lew K K, Redwing J M and Mallouk T E 2007 *JACS* **129** 12344–12345

[7] Muskens O L, Borgström M T, Bakkers E P A M and Rivas J G 2006 *Appl. Phys. Lett.* **89** 233117

[8] Sköld N, Karlsson L S, Larsson M W, Pistol M E, Seifert W, Trägårdh J and Samuelson L 2005 *Nano Lett.* **5** 1943–1947

[9] Nicorovici N A, McKenzie D R and McPhedran R C 1995 *Optics Comm.* **117** 151–169

[10] Hodgkinson I J and Wu Q H 1997 *Birefringent Thin Films and Polarizing Elements* (World Scientific)

[11] Stefano L D, Rendina I, Moretti L, Tundo S and Rossi A M 2004 *Applied Optics* **43** 167–172

[12] Gross E, Kovalev D, Künzner N, Timoshenko V Y, Diener J and Koch F 2001 *J. Appl. Phys.* **90** 3529–3532

[13] Künzner N, Gross E, Kovalev D, Timoshenko V Y and Wallacher D 2003 *J. Appl. Phys.* **94** 4913–4917

[14] Lin V S Y, Motesharei K, Dancil K P S, Sailor M J and Ghadiri M R 1997 *Science* **278** 840–843

[15] Dancil K P S, Greiner D P and Sailor M J 1999 *JACS* **121** 7925–7930

[16] Létant S E and Sailor M J 2001 *Adv. Mat.* **13** 335–338

[17] Stewart M P and Buriak J M 2000 *Adv. Mat.* **12** 859–869

[18] Stefano L D, Arcari P, Lamberti A, Sanges C, Rotiroti L, Rea I and Rendina I 2007 *Sensors* **7** 214–221

[19] Saarinen J J, Weiss S M, Fauchet P M and Sipe J E 2005 *Optics Express* **13** 3754–3764

[20] Snow P A, Squire E K and Russell P S J 1999 *J. of Appl. Phys.* **86** 1781–1784

[21] Ouyang H, Striemer C C and Fauchet P M 2006 *Appl. Phys. Lett.* **88** 163108

[22] Schulz B, Chan D, Bäckström J and Rübhausen M 2004 *Thin Solid Films* **455-456** 731–734

[23] Wagner R and Ellis W 1964 *Appl. Phys. Lett.* **4** 89

[24] Hannon J B, Kodambaka S, Ross F M and Tromp R M 2006 *Nature* **440** 69

[25] Björk M T, Ohlsson B J, Sass T, Persson A I, Thelander C, Magnusson M H, Deppert K, Wallenberg L R and Samuelson L 2002 *Nano Lett.* **2** 87

[26] Huang M H, Mao S, Feick H, Yan H, Wu Y, Kind H, Weber E, Russo R and Yang P 2001 *Science* **292** 1897

[27] Duan X, Huang Y, Agarwal R and Lieber C M 2003 *Nature* **421** 241–245

[28] Muskens O L, Diedenhofen S L, van Weert M H M, Borgström M T, Bakkers E P A M and Rivas J G 2008 *Adv. Func. Mat.* **18** 1039

[29] Oton C J, Gaburro Z, Ghulinyan M, Pancheri L, Bettoti P, Negro L D and Pavesi L 2002 *Appl. Phys. Lett.* **81** 4919–4921

[30] Kirchner A, Busch K and Soukoulis C M 1998 *Phys. Rev. B* **57** 277–288

[31] Rivas J G, Muskens O L, Borgström M T, Diedenhofen S L and Bakkers E P A M 2008 *One-Dimensional Nanostructures* (*Lecture Notes in Nanoscale Science and Technology* vol 3) (Springer)